

3-22-2022

## Cyclotron mass of an electron in strong magnetic fields in a wide InAs quantum well

B. T. Abdulazizov

Follow this and additional works at: <https://www.ephys.kz/journal>

---

### Recommended Citation

Abdulazizov, B. T. (2022) "Cyclotron mass of an electron in strong magnetic fields in a wide InAs quantum well," *Eurasian Journal of Physics and Functional Materials*: Vol. 6: No. 1, Article 3.

DOI: <https://doi.org/10.32523/ejpfm.2022060103>

This Original Study is brought to you for free and open access by Eurasian Journal of Physics and Functional Materials. It has been accepted for inclusion in Eurasian Journal of Physics and Functional Materials by an authorized editor of Eurasian Journal of Physics and Functional Materials.

# Cyclotron mass of an electron in strong magnetic fields in a wide InAs quantum well

B.T. Abdulazizov

Physical-Technical Institute Uzbekistan Academy of Sciences, Tashkent, Uzbekistan

Namangan State University, Namangan, Uzbekistan

E-mail: abdulazizovbahromjon@gmail.com

DOI: 10.32523/ejpfm.2022060103

Received: 25.02.2022 - after revision

The results of calculations of the Landau level and cyclotron mass in strong magnetic fields in an InAs quantum well based on the two-band model are presented. The calculations were performed in the approximation of infinity of the depth of the quantum well, taking into account the Landau level of the second subband. It is shown that taking into account the cyclotron transition of electrons within the second subband satisfactorily describes the experimental data obtained in strong magnetic fields in the  $InAs/In_{0.81}Ga_{0.19}As/In_xAl_{1-x}As$  heterostructure.

**Keywords:** InAs; heterostructure; quantum well; subbands; nonparabolic dispersion; two band model; Kane model; Landau levels; two dimensional electron gas; effective mass; cyclotron mass; cyclotron resonance

## Introduction

Conduction electrons in a narrow-gap semiconductor InAs have a small effective mass [1] ( $m^* \approx 0.023 \div 0.03m_0$ ) and, therefore, a high mobility. Therefore, InAs-based quantum wells (QW) formed in various heterostructures (HS) are promising for creating new generation electronic and optoelectronic devices [2-4], technologies for obtaining InAs based heterostructures are widely described [5-8]. Cyclotron resonance (CR) is one of the effective methods for studying the band structure and spectrum of carriers in QWs. The CR can be used to reveal the

nonparabolicity of the dispersion law and obtain information about the features of the zone of new materials. In weak magnetic fields, the effective carrier mass at the Fermi level can be determined. In strong (quantizing) magnetic fields, this method makes it possible to determine the distance between Landau levels (cyclotron energy) between which optical transitions occur and thereby obtains a cyclotron mass [9-12].

In a two-dimensional electron gas, the energy levels of electrons lie far from the bottom of the conduction band, which is especially important for the nonparabolicity of the dispersion law. Application of a strong magnetic field leads to a large value of the cyclotron and Zeeman energies [9].

The study of the properties of current carriers in strong magnetic fields in QWs based on InAs continues today [13, 14]. The results of such studies can be applied to various technological developments.

In [14], InAs QWs based on structure InAs/In<sub>0.81</sub>Ga<sub>0.19</sub>As/In<sub>x</sub>Al<sub>1-x</sub>As ( $x = 0.52-0.81$ ) were studied. The CR was used to measure the effective mass of the  $m_{CR}$  and  $g_{CR}$  – factor of the electron at strong magnetic fields (up to 70 T) and at different temperatures. The experimental results were interpreted qualitatively on the basis of the two-band Kane model and in the QW model of infinite depth, however, no quantitative comparison was made.

In strong magnetic fields and in wide QWs, the Landau levels of different subbands can approach or overlap sufficiently. Mathematical modeling of such processes using experimental values of  $m_{CR}$  and  $g_{CR}$  makes it possible to better understand the band structure and the location of the Landau levels of the 1st and 2nd minibands.

The aim of this work is to calculate the Landau levels of the 1st and 2nd subbands and, on the basis of these data, the dependence of the cyclotron mass  $m_{CR}$  on the magnetic field is determined. The calculations will be carried out on the basis of the two-band Kane model and the QW model of infinite depth. On the basis of these calculations, possible interpretations of the experimental results are discussed [14].

## Basic formulas

Let us consider the motion of one electron in the QW conduction band. Then, in the presence of a magnetic field applied perpendicular to the QW plane, the electron spectrum can be represented as [9, 15] (two-band model)

$$\varepsilon \left( 1 + \frac{\varepsilon}{\varepsilon_g} \right) = \frac{m_0}{m_n} \left[ \left( N + \frac{1}{2} \right) \hbar\omega_0 + \frac{\hbar^2 k_z^2}{2m_0} \right] + \frac{g_n}{g_0} \sigma \hbar\omega_0. \quad (1)$$

Here,  $\varepsilon_g$  is the band gap,  $m_n$  and  $g_n$  are the effective mass and the spin splitting factor at the bottom of the conduction band,  $m_0$  and  $g_0 = 2$  are the mass and the spin splitting factor of a free electron, respectively,  $N$  – is the Landau level number,  $\sigma$  – is the  $\pm 1/2$  spin index,  $\hbar\omega_0$  – is the cyclotron energy of free electron

$$\hbar\omega_0 = \hbar \frac{eB}{m_0} = 1.16 \times 10^{-4} B \left[ \frac{eV}{T} \right]. \quad (2)$$

In the QW, the electron motion in the  $z$  direction is also quantized. For example, in the QW model with an infinite potential barrier  $V = \infty$ , and width  $L$ , the value of the wave vector  $k_z$  in equation (1) is equal to  $k_z = \pi n/L$ ,  $n$  is the number of the spatial quantization level.

According to equations (1) and (2), the electron spectrum depends on the magnitude of the magnetic field  $B$ , the number of the spatial quantization level  $n$ , the number of the Landau level  $N$ , and the spin index  $\sigma$ . The cyclotron mass is determined by the equation [9, 15]

$$\frac{m_0}{m_{CR}(B)} = \frac{\varepsilon(n, N+1, \sigma) - \varepsilon(n, N, \sigma)}{\hbar\omega_0}. \quad (3)$$

The chemical potential and the fraction of electrons in the Landau levels can be found from the equation

$$\begin{aligned} n_S &= \frac{eB}{\pi\hbar} \frac{1}{2} \sum_{n,N,\sigma} f(\varepsilon(n, N, \sigma), \mu, T) = \\ &= D_0 \hbar\omega_0 \frac{1}{2} \sum_{n,N,\sigma} \frac{1}{\exp[(\varepsilon(n, N, \sigma) - \mu)/T] + 1}. \end{aligned} \quad (4)$$

where,  $\mu$  – is the chemical potential,  $f(\varepsilon(n, N, \sigma), \mu, T)$  – is the Fermi-Dirac distribution function.  $T$ , [eV] denotes the quantity  $k_B T$ ,  $k_B$  – is the Boltzmann constant,  $D_0 = m_0/\pi \hbar^2 = 413 \cdot 10^{12} / \text{eV} \cdot \text{cm}^2$

## Dependence of the cyclotron mass on the magnetic field

As seen from equation (3), to calculate the dependence  $m_{CR}(B)$ , it is necessary to know the Landau levels  $\varepsilon(n, N, \sigma)$ , which can be found from equation (1). Therefore, first we plot the field dependence of the Landau levels  $\varepsilon(n, N, \sigma)$ . The band parameters of InAs used in the calculations is given in Table 1. The experimental value of the electron concentration in the sample where the  $m_{CR}(B)$  dependence was investigated is also given [14].

Table 1.

Band parameters of InAs QW.

$E_g$ , [eV]	0.42
$m_n$ , [ $m_0$ ]	0.023
$g_n$	-15
$L$ , [nm]	20
$n_S$ , [ $\text{cm}^{-2}$ ]	$3.6 \times 10^{11}$

The calculated field dependences of the Landau level  $\varepsilon(n, N, \sigma)$  and the Fermi energy for InAs QWs of width  $L = 200 \text{ \AA}$  are shown in Figure metricconverter-ProductID1. In1. In calculating the Fermi energy from equation (4), we assumed  $T = 20.5 \text{ K}$  and  $n_S = 3.6 \times 10^{11} \text{ cm}^{-2}$ .

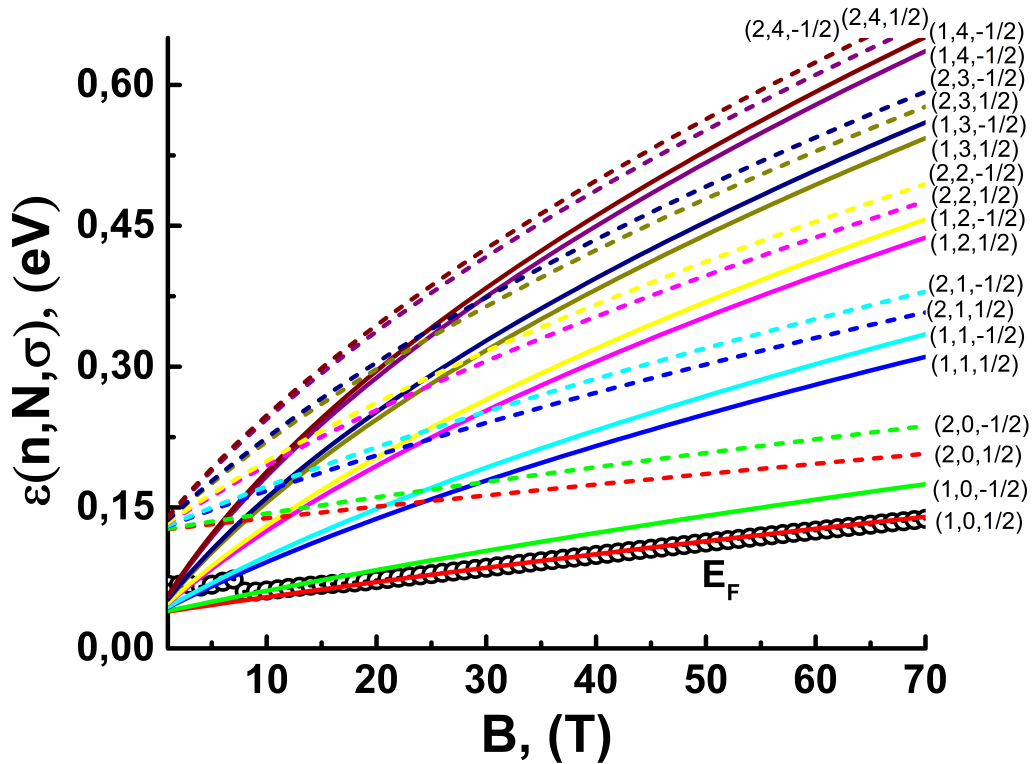


Figure 1. Electron Landau levels and Fermi energy in InAs QW with  $L = 20$  nm depending on the magnetic field. Solid lines – levels for the first subband, dashed lines – for the second subband. The thick line is the Fermi energy calculated from equation (4) at  $T = 20.5$  K and  $n_s = 3.6 \times 10^{11} \text{ cm}^{-2}$ .

It can be seen from the graph that, the ground level with  $n = 1$ ,  $N = 0$  approximately linearly depends on the magnetic field  $B$ , and the upper lines differ markedly from the linear law, which is due to the nonparabolicity of the conduction band. Starting from approximately  $B \sim 30$  T, the ground Landau level of the second subband lies lower than the second Landau level of the first subband, i.e.  $\varepsilon(2,0,\sigma) < \varepsilon(1,1,\sigma)$ . Then, at high temperatures and strong fields ( $B > 30$  T), the  $\varepsilon(2,0,\sigma)$  level can mainly be partially populated. As can be seen from the graph, in strong fields ( $B > 30$  T) all electrons lies at the level  $\varepsilon(1,0,1/2)$ .

Figure 2 shows comparisons of the results of the calculation of  $m_{CR}$  with the experimental points [14] obtained at the temperature  $T = 20.5$  K.

As can be seen from Figure 2, the lower three experimental points are well described by the considered model as the cyclotron transition  $(1,0,\sigma) \rightarrow (1,1,\sigma)$ .

It should be noted that at temperature  $T = 20.5$  K, the Landau levels  $\varepsilon(1,1,\sigma)$  or  $\varepsilon(2,0,\sigma)$  cannot be populated, since, in this case, the thermal energy  $k_B T \sim 0.0018$  eV is much less than the differences  $\varepsilon(1,1,\sigma) - \varepsilon(1,0,\sigma)$  or  $\varepsilon(2,0,\sigma) - \varepsilon(1,0,\sigma)$ .

However, if we assume the presence of electrons with a long lifetime that hit the level  $\varepsilon(2,0,\sigma)$  upon photoexcitation, then the origin of the three experimental points can be explained by cyclotron transitions  $(2,0,\sigma) \rightarrow (2,1,\sigma)$ . This is seen from Figure 2, where the calculated points are shown by dashed lines.

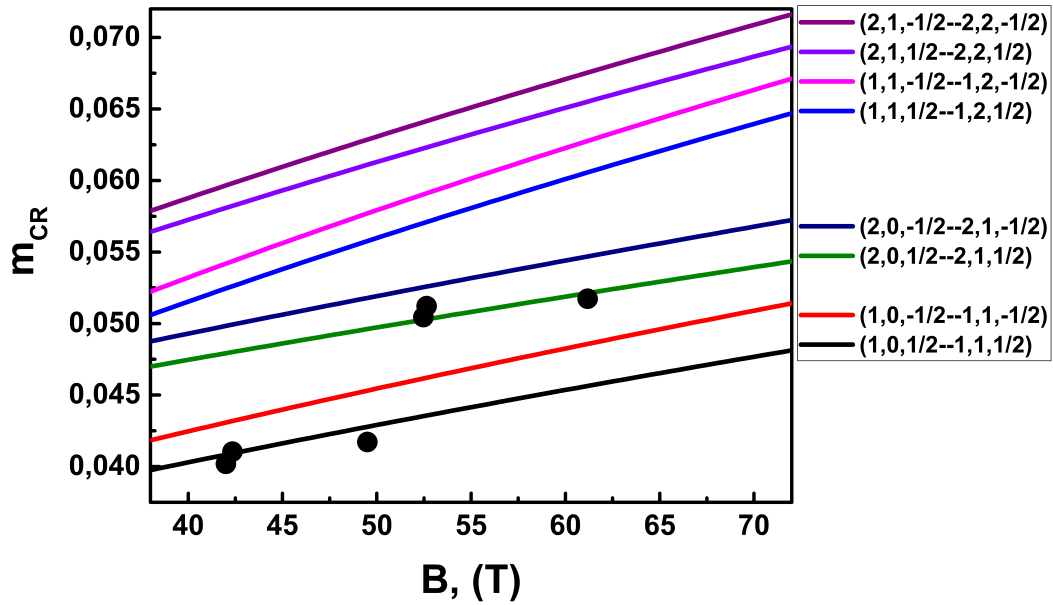


Figure 2. Comparisons of the field dependence of the cyclotron mass  $m_{CR}$  with the experimental points [14] obtained at temperature  $T = 20.5$  K. Calculations were performed for InAs QWs with  $L = 20$  nm. The numbers indicate interlevel transitions, see equation (3).

## Conclusion

Calculations showed that when interpreting experimental data, taking into account the Landau levels of the second subband is also important. It turned out that, within the framework of the simple model under consideration, the experimental points  $m_{CR}(B)$  measured at temperature  $T = 20.5$  K are associated with cyclotron transitions  $(1,0,\sigma) \rightarrow (1,1,\sigma)$  and  $(2,0,\sigma) \rightarrow (2,1,\sigma)$ . The correct picture is restored when the model explains the concentration and field dependences of the Shubnikov-de-Haas oscillations, optical transmissions, cyclotron mass and g-factors measured experimentally [14]. This requires solving problems taking into account the finiteness of the QW depth in the heterostructure InAs/In<sub>0.81</sub>Ga<sub>0.19</sub>As/In<sub>x</sub>Al<sub>1-x</sub>As.

## Acknowledgments

The work was financially supported by the Fundamental Research Grant FZ-20200929243 "The Effect of Hot Electrons and Phonons in a Strong Electromagnetic Field on the Characteristics of Semiconductor Solar Photovoltaic Elements and Nanostructures".

## References

- [1] I. Vurgaftman, J. R. Meyer, and L. R. Ram-Mohan, J. Appl. Phys. **89** (2001) 5815. [[CrossRef](#)]
- [2] B.R. Bennett et al., Appl. Phys. Lett. **72** (1998) 1193. [[CrossRef](#)]
- [3] R. Magno et al., Journal of Applied Physics **89** (2001) 5791. [[CrossRef](#)]

- [4] T. Yu et al., J. Semiconductors, **39** (2018) 114003. [[CrossRef](#)]
- [5] X. Wallart et al., Appl. Phys. Lett. **87** (2005) 043504. [[CrossRef](#)]
- [6] J. Shabani et al., Appl. Phys. Lett. **105** (2014) 262105. [[CrossRef](#)]
- [7] J. Shabani et al., Phys. Rev. B **90** (2014) 161303(R). [[CrossRef](#)]
- [8] R.Z. Bakhtizin et al., Journal of Experimental and Theoretical Physics **91** (2000) 1000-1010. [[CrossRef](#)]
- [9] I.M. Tsidilkovsky, Electrons and holes in semiconductors. Chapter 6 (Nauka, Moscow, 1972) 526 p. (in Russian)
- [10] A. Mrenca-Kolasinska, K. Kolasinski, and B. Szafran, Phys. Rev. B **98** (2018) 115309. [[CrossRef](#)]
- [11] G. Gulyamov, B.T. Abdulazizov, P.J. Baymatov, Journal of Nanomaterials (2021) 5542559. [[CrossRef](#)]
- [12] B.T. Abdulazizov et al., SPIN **12**(1) (2022) 2250002-1. [[CrossRef](#)]
- [13] H. Arimoto et al., Phys. Rev. B **67** (2003) 155319. [[CrossRef](#)]
- [14] J. Yuan et al., Phys. Rev. B **101** (2020) 205310. [[CrossRef](#)]
- [15] R. Winkler, Spin-Orbit Coupling Effects in Two-Dimensional Electron and Hole Systems (Springer Verlag, Berlin Heidelberg, 2003) 236 p.